

Article

Effect of Mean Velocity to Critical Velocity Ratios on Bed Topography and Incipient Motion in a Meandering Channel: Experimental Investigation

Nargess Moghaddassi ¹, Seyed Habib Musavi-Jahromi ^{2,*}, Mohammad Vaghefi ³ and Amir Khosrojerdi ⁴

¹ Ph.D. Student, Department of Water Engineering, Science and Research Branch, Islamic Azad University, Tehran, Iran; Email: nargess.moghaddassi@srbiau.ac.ir. ORCID: 0000-0002-6442-6380

² Emeritus Professor of Hydraulic Structures, Faculty of Water Sciences Engineering, Shahid Chamran University of Ahwaz, Ahwaz, Iran; Email: h-mousavi@srbiau.ac.ir. ORCID: 0000-0002-9450-460X

³ Associate Professor of Hydraulic Structures, Department of Civil Engineering, Persian Gulf University, Bushehr, Iran; Email: vaghefi@pgu.ac.ir. ORCID: 0000-0001-5862-915X

⁴ Assistant Professor of Hydraulic Engineering, Department of Water Engineering, Science and Research Branch, Islamic Azad University, Tehran, Iran; Email: khosrojerdi@srbiau.ac.ir.

* Correspondence: h-mousavi@srbiau.ac.ir; Tel.: +989127126513

Abstract: As 180-degree meanders are observed in abundance in nature, a meandering channel with two consecutive 180-degree bends was designed and constructed to investigate bed topography variations. These two 180-degree mild bends are located between two upstream and downstream straight paths. In this study, different mean velocity to critical velocity ratios have been tested at the upstream straight path to determine the meander's incipient motion. To this end, bed topography variations along the meander and the downstream straight path were addressed for different mean velocity to critical velocity ratios. In addition, the upstream bend's effect on the downstream bend has been investigated. Results indicated that the maximum scour depth at the downstream bend has increased as a result of changing the mean velocity to critical velocity ratio from 0.8 to 0.84, 0.86, 0.89, 0.92, 0.95, and 0.98 by respectively 1.5, 2.5, 5, 10, 12, and 26 times. Moreover, increasing the ratio increased the maximum sedimentary height by 3, 10, 23, 48, 49, and 56 times. The upstream bend's incipient motion was observed for the mean velocity to critical velocity ratio of 0.89, while the downstream bend was equal to 0.78.

Keywords: 180-degree bend, Sediment transport, Clear water, Open-channels, Scour

1. Introduction

Seldom can rivers in nature be observed to be following a straight path, and they tend to flow in meandrous or braided patterns. The presence of meanders [1,2] in river paths is a factor involved in creating scour or sedimentation. On the other hand, hydrodynamic forces are applied onto sediment particles on the river bed through the river path. An increase in flow velocity augments the hydrodynamic forces. Thus, if the flow force can overcome bed sediments' weight force, this process will result in sediment transport [3] and bed topography variations. As a result of the interaction between the longitudinal and secondary flows in bent paths and the generation of helical flows [4], the flow's force becomes more complex. This leads to more sediment transport than that occurring in upstream straight paths. Hence, studying and understanding sediment transport and sediment incipient motion mechanisms in bends require more investigation than straight channels.

A great number of research studies have so far been conducted with regards to incipient motion in rivers due to its importance, and the following research works may be referred to as instances:

Shields [5] defined the incipient motion based on the sediment transport rate. Inspired by the studies conducted by Shields, Dey and Papanicolaou [6] carried out advanced studies to determine the incipient motion under the influence of a steady flow. Kramer [7] discussed the sediment incipient motion particles based on the apparent condition of particle motion. Bagnold [8] described the incipient motion based on the uplift force. Neill [9] defined the incipient motion based on the critical velocity. Lavelle and Mofjeld [10] examined the concept of critical stress under incipient motion conditions in a turbulent flow. The results obtained from their studies suggest that there is no specific definition of a process that leads to scouring because the researcher discerns the time and the extent of sediment transport as both effective and important, which can be enough to bring about much uncertainty about this phenomenon. Yen and Lee [11] investigated bed topography variations in a 180-degree mild bend under unsteady flow conditions. Their research refers to the significant effect of the secondary flow and velocity at the outer bend on bed topography variations. Dey and Debnath [12] evaluated the effect of bed slope on sediment particle motion. After analytical and experimental investigations and the application of different static angles for sediments, they concluded that the critical shear stress decreased with an increase in bed slope. Xu and Bai [13] conducted an empirical study on bed topography formation in alluvial and meandering rivers with different radii. To study the role of different sinusoidal shapes of the channels on the flow variations and the bed morphology in meandering rivers, they carried out their experiments in curved channels with fixed walls and movable bed. Mohtar [14] studied the effect of turbulent fluctuations and vortices on the sediment incipient motion. Their results implied a constant Shields parameter in the flow region having a rigid bed. Having addressed the flow velocity direction in meandering channels, Liu et al. [15] developed a model for calculating the mean 2D flow velocity. Qin et al. [16] investigated the secondary flow effect on bed topography variations and cohesive sediment transport in Yangtze's meandering path. Azarisamani et al. [17] worked on the effect of rigid vegetation on bed topography variations and flow velocity in a meandering channel.

Most studies on the incipient motion have so far been conducted in totally straight or single-bended paths, as noted above. Hence, the present work has addressed the effect of variations in the mean velocity (U) to critical velocity (U_c) ratios (U/U_c) [18] at the upstream straight path on bed topography along the meandering channel (with two consecutive 180-degree bends connecting two straight paths). Furthermore, the effect of the upstream bend geometry on bed topography variations in the downstream bend and the influence of the downstream straight path on the upstream bend have been analyzed. Determining the sediment incipient motion conditions in both bends were among the other highlights in this study.

2. Materials and Methods

In order to carry out the intended experiments in the laboratory, the meandering channel with two consecutive bends, as shown in Figure 1, was designed, implemented, and constructed for the first time in Iran [19]. This channel is composed of an 8-meter-long path upstream and one downstream, connected by two consecutive 180-degree bends with inner and outer radii of 3 and 4 meters. The channel wall is 80 cm high and 100 cm wide, and the ratio of the bend radius (R) to channel width (B) is equal to $R/B=3.5$. According to the categorization developed by Leschziner and Rodi [20], this bend qualifies as a mild bend.

As Raudkivi and Ettema [21] recommended, the mean particle diameter (d_{50}) must be larger than 0.7 mm to prevent dunes formation [22]. Hence, the channel bed is covered with a 30-cm-thick layer of silica sand with $d_{50}=1.85$ mm and a standard deviation of 1.2. Given the criterion suggested by Chiew [23], the tests were considered to run for 4 hours. To supply the required water to the channel, side reservoir tanks with a capacity of 30 m³ have been used. The discharge capacity produced by the pump system has been constantly 70 Lit/s when running the tests. The ultrasonic Aktek (Type: TFM3100-F1)

flowmeter with a precision of $\pm 1\%$ was utilized for determining the discharge. The flow depth at the upstream straight path was considered to range from 17 to 21.8 cm to provide flow velocity variations under incipient motion conditions. Mean velocity to critical velocity ratios (U/U_c) were determined from 0.75 to 0.98 at the upstream straight path, considering the formula proposed in Neill [9] and a constant discharge. Therefore, the Froude number falls within the range of 0.22 to 0.31 and is subcritical in different tests.

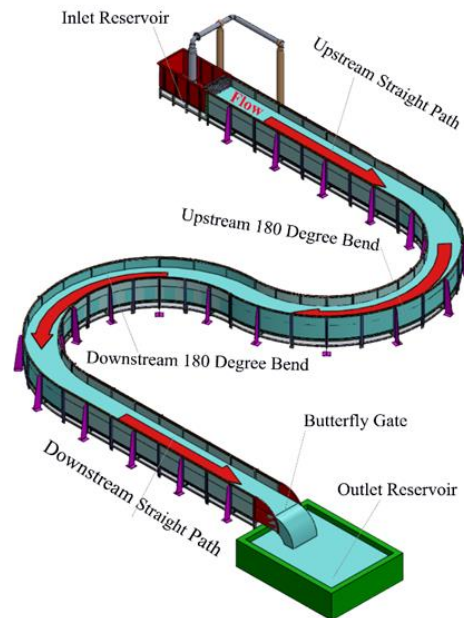


Figure 1. Schematic 3D view of the meandering channel.

In these tests, the Leica laser bathometer (DISTO-D510) with a precision of 1 mm in 200 meters has been used for bed topography data collection. The mesh grid for data collection covered the area from the beginning of the first bend to the end of the second bend at 1-cm intervals at the width and specific angles. Given the importance of data collection in the range of the connection between the two bends and their downstream area, smaller angles than the upstream path have been used for the mesh grid.

3. Results

3.1. Bed Topography Variations

This section aims to provide the incipient motion for upstream and downstream bends regarding variations in U/U_c at the upstream straight path. Bed topography variations in tests with U/U_c ranging from 0.75 to 0.86 have been presented in Figure 2. One important note considered here is the effect of the upstream bend geometry and the flow passing through it on bed topography variations at the downstream bend. As it may be observed in Figure 2-a ($U/U_c=0.75$), bed topography has remained unchanged from the beginning of the upstream bend to the end of the downstream bend. Neither of the bends has reached the incipient motion condition yet. In Figure 2-b, the onset of bed topography variations occurs at the downstream bend after changing U/U_c from 0.75 to 0.8. These variations reach a maximum within the range of 200 to 300 degrees, and sediment transport has been observed in groups of 5 to 20 particles. Moreover, the incipient motion at the downstream bend happened as $U/U_c=0.78$ at the straight path upstream. As shown in this figure, the maximum scour depth, equivalent to $0.32d_{50}$ (0.6 cm), occurs at the 275-degree angle.

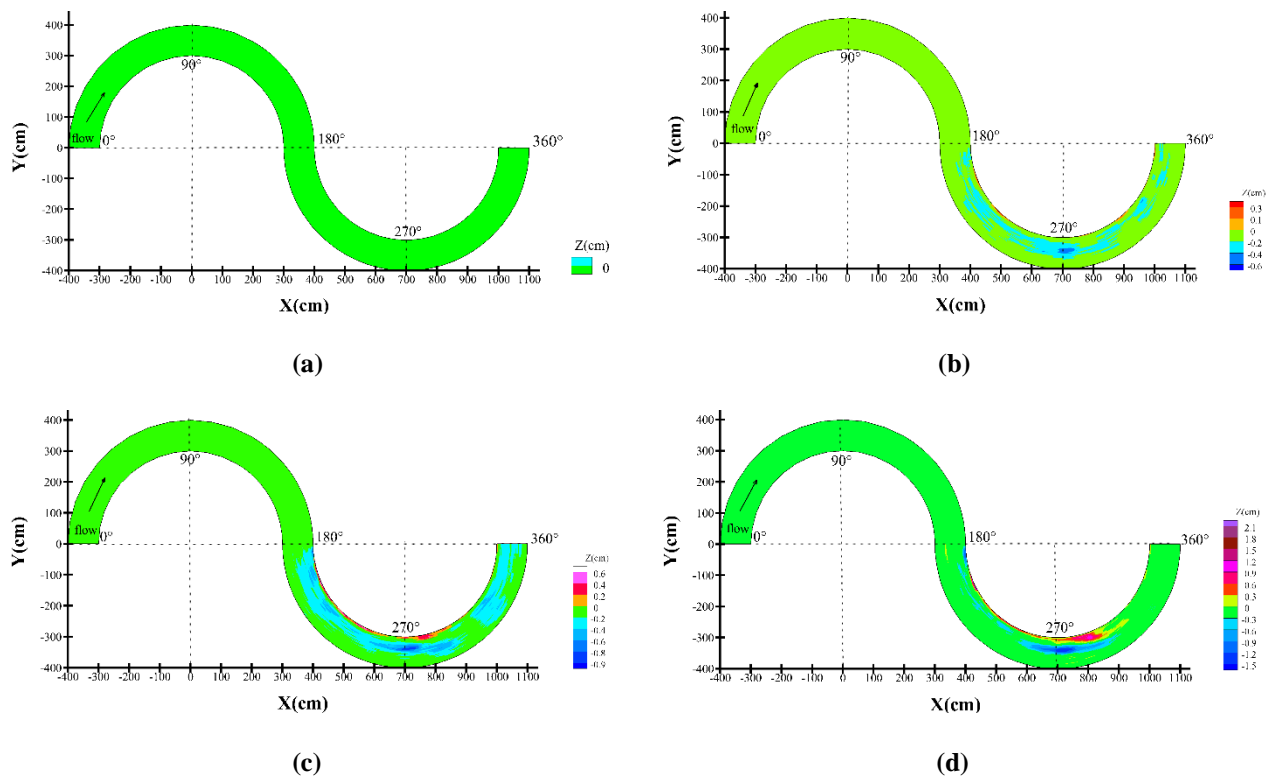


Figure 2. Bed topography variations for different U/U_c values: (a) 0.75, (b) 0.8, (c) 0.84, and (d) 0.86.

The maximum sedimentation height has also been developed insignificantly at the 200-degree angle. In Figure 2-c, the region with the maximum bed topography variations is observable from approximately the 195 to 300-degree angles following an increase in U/U_c from 0.8 to 0.84. The maximum scour depth and sedimentation height have occurred at $0.48d_{50}$ (0.9 cm) at the 275-degree angle and $0.32d_{50}$ (0.6 cm) at the 195-degree angle. With the increase in U/U_c from 0.8 to 0.84, there has been no significant change in bed topography at the upstream bend; however, the maximum scour depth and sedimentation height at the downstream bend have respectively increased by 1.5 and 3 times. The maximum scour occurs at mid-channel in the 275-degree cross-section, and the maximum sedimentation is observed at a distance of 5% of the inner bend around the 195-degree angle. As it may be observed in Figure 2-d ($U/U_c=0.86$), the secondary flow strength at the upstream bend is not high enough to alter bed topography, yet bed topography variations are evident from 200 to 300 degrees. The maximum scour and sedimentation have also occurred for $0.8d_{50}$ at 275 degrees and $1.14d_{50}$ at 200 degrees. In fact, by increasing the U/U_c range of 0.84-0.86, there has been an increase of 1.5 and 3.5 times in the maximum scour and sedimentation, respectively. The flow velocity has grown at the downstream bend given the decline in the water height under the downstream straight path's effect. Hence, bed topography undergoes some changes. The flow at the upstream bend is directed towards the inner bank in the first half. When the flow reaches the second half of the bend, it is diverted first towards mid-channel and then towards the outer bank. With the augmentation of the secondary flow strength at the sections towards the end of the upstream bend, the scour onset also spreads to the beginning of the downstream bend for this U/U_c . There has been a conversion at the junction between the two bends. Therefore, the outer bank at the upstream bend has become the inner bank at the downstream bend, which causes a change of directions in the secondary flows.

A comparison between different conditions illustrated in Figure 2 suggests that the maximum sedimentation height for each of these cases has occurred from 195 to 200 degrees at a distance equal to 5% of the inner bank's channel width. This may be attributed

to the sediment transport's direction towards the inner bank under the secondary flow pattern's influence. Furthermore, considering the secondary flow direction, the flow's shedding over the sediments, and the generation of a downflow, the maximum scour has occurred in the second half of the downstream bend around the 275-degree angle and mid-channel in every test.

Bed topography variations have been shown in Figure 3 in tests with U/U_c values ranging from 0.89 to 0.98. As shown in Figure 3-a ($U/U_c=0.89$), the secondary flow strength in the first half of the upstream bend is not high enough to cause a change in bed topography. On the other hand, the variations occur trivially in the second half of the bend from 170 to 180 degrees at the outer bank so that the maximum scour depth, 0.8 cm, has occurred at the 180-degree angle. This can be taken as the incipient motion condition described at the upstream bend in the meandering channel. In other words, when U/U_c is 0.89 at the upstream straight path, the first bend hosts the incipient motion condition. The upstream bend's effect on the downstream bend is mainly due to an increase in the secondary flow strength, which breeds variations in topography, clearly observable at the downstream bend. Hence, bed topography variations at the downstream bend have reached a maximum from 200 to 300 degrees, and the maximum scour depth, equivalent to $1.62d_{50}$ (3 cm), has occurred at the 275-degree angle. The maximum sedimentation height, equivalent to $2.5d_{50}$ (4.6 cm), has also been realized at the 200-degree angle. Moreover, increasing U/U_c from 0.86 to 0.89 has doubled the maximum scour depth and sedimentation height. In Figure 3-b, the bed topography remains unchanged at the first half of the upstream bend, but more changes are observed in the second half at the outer bank from 170 to 180 degrees. The flow and scour patterns hitherto described suggest a resemblance between the results of this work and those of other researchers [13,24] in a small-scale laboratory model of a meandering channel. As shown in this figure, the maximum scour depth, equivalent to $1.84d_{50}$ (3.4 cm), has occurred at the 180-degree angle. Further, a 3.4% increase in U/U_c has also raised the maximum scour depth at the end of the outer bend at the upstream bend by approximately a factor of 4. In addition, the largest bed topography variations at the downstream bend have occurred within the range of 200 to 300 degrees, where the maximum scour depth, equal to $3.24d_{50}$ (6 cm), has been developed at the 190-degree angle. In this case, the maximum sedimentation height, equal to $5.2d_{50}$ (9.6 cm), was observed at the 220-degree angle. On the other hand, an increase in U/U_c at the upstream straight path resulted in doubled values of the maximum scour depth and sedimentation height reported. In Figure 3-c ($U/U_c=0.95$), the entrance of the flow into the first bend has led to insignificant variations in bed topography at the first half of the upstream bend, while it has created scour at the second half of the bend from 170 to 180 degrees at the outer bank. The maximum scour depth, equal to $1.9d_{50}$ (3.5 cm), has occurred at the 180-degree angle. As with the previous cases, the maximum bed topography variations at the downstream bend have occurred from 200 to 300 degrees. This region hosts the greatest secondary flow strength and the influence of the helical flow in the bend. Such a strong flow stems from the helical flow present inside the downstream bend itself, and its excessive increase is a consequence of the upstream bend geometry's affecting the downstream bend. Here, the maximum scour depth and sedimentation height, respectively equal to $3.9d_{50}$ and $5.3d_{50}$ (corresponding to 7.2 cm and 9.8 cm), have occurred at 195 and 225 degrees. Considering the explanations provided in this figure, it can be concluded that increasing U/U_c has not increased the maximum scour depth at the upstream bend and the maximum sedimentation height at the downstream bend. On the other hand, the maximum scour depth at the downstream bend has been developed by 1.2 times at a distance of 5 to 10 degrees from the beginning of the bend under the influence of the shift in the flow direction at the junction of the two bends.

A comparison of bed topography variations in a single 180-degree sharp bend for $R/B=2$ and $U/U_c=0.96$ in an experimental study by Vaghefi et al. [25] and a numerical study by Asadollahi et al. [26] with the results observed at the downstream bend in Figure 3-c was made.

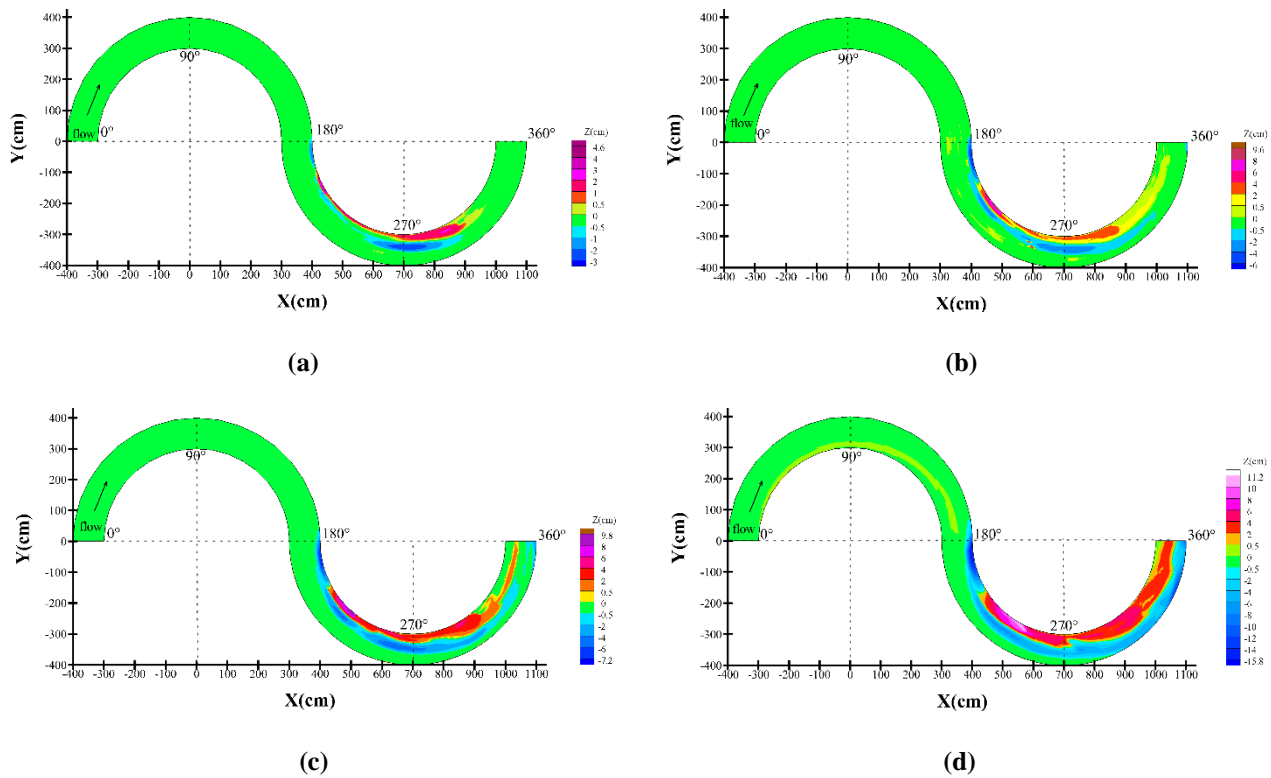


Figure 3. Bed topography variations for different U/U_c values: (a) 0.89, (b) 0.92, (c) 0.95, and (d) 0.98.

The results of this comparison indicate that in both channels, whether with sharp or with mild bends, sedimentation begins at the inner bends from approximately 30 degrees. In the present study, given the use of mild bends, there are trivial variations of sedimentation observed at the upstream bend's inner wall. Still, the intensity of sedimentation is greater in a sharp bend. Besides, an investigation of the scour pattern at the downstream meandering bend in comparison with the 180-degree sharp bend refers to the resemblance of the scour pattern in the middle of the bend in both cases; however, the maximum scour at the 180-degree sharp bend occurs from 40 to 80 degrees, whereas that in the meandering channel has occurred at the 190-degree angle in the vicinity of the inner wall under the influence of the flows approaching from the upstream bend. These observations are also in line with investigations of Termini [24] in a meandering channel with consecutive bends on the maximum scour, which occurred at the second inner bend downstream.

In Figure 3-d ($U/U_c=0.98$), illustrating the bed materials incipient motion at the upstream straight path, it may be observed that the flow velocity and strength have risen. Moreover, given the streamlines at the bed, extended from the outer bank towards the inner bank, the inner bank at the first half of the bend first undergoes sedimentation, but the sedimentation variations in the first half are trivial since the bend is mild. As the secondary flow in the second half of the upstream bend is directed towards the outer bank, as with the previous cases, the maximum scour has occurred at the outer bank between 170 and 180 degrees. The maximum scour depth, equal to $6.5d_{50}$ (12.1 cm), was found at the 178-degree angle. Bed topography variations at the downstream bend also reached the maximum between 200 and 300 degrees; the maximum scour depth and sedimentation height, separately equal to $8.5d_{50}$ and $6.05d_{50}$ (15.8 and 11.2 cm), have respectively occurred at 195 and 240 degrees. A comparison between Figures 3-c and 3-d indicates that for a change in U/U_c from 0.95 to 0.98, the maximum scour depth at the upstream bend has

increased by 3.5 times. Also, at the downstream bend, the maximum scour depth and sedimentation height have respectively increased by 2.2 and 1.1 times.

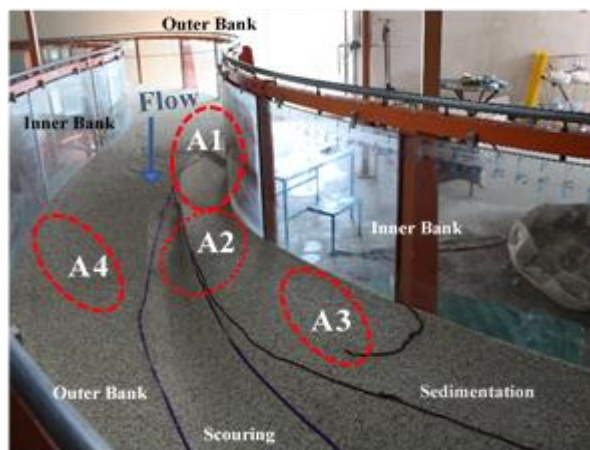
In general, a comparison made between different cases presented in Figure 3 suggests that a decline in the water level and an increase in velocity have happened given the straight downstream path's effect and its effect on the meander (particularly on the second half of it). This has entailed further bed topography variations at the downstream bend, more specifically at the second half. Also, the downstream bend functioned as an obstacle against the flow present at the upstream bend. Such behavior has resulted in fewer bed topography variations observed at the upstream bend than those at the downstream bend. A review of the general bed topography variations illustrated in Figures 2 and 3 explains why the maximum scour occurred at a distance of 5% from the outer bank between 178 and 180 degrees for every U/U_c value at the upstream bend. The maximum scour location at the downstream bend has changed due to the influence of the upstream bend on the downstream bend and the increase in its velocity. As observed, from $U/U_c=0.8$ to $U/U_c=0.89$, the maximum scour has occurred at distances of 30 to 40% of the channel width between 270 and 275-degree angles, whereas from $U/U_c=0.92$ to $U/U_c=0.98$, the maximum scour has occurred at a distance of 5% from the inner bank between 185 and 195-degree angles. Furthermore, since the flow in the first half of the downstream bend is directed towards the inner bank, the maximum sedimentation volume has also occurred at a distance from 0 to 5% of channel width from the inner bank for all cases. Increasing U/U_c from 0.8 to 0.98 has changed the location of the maximum sedimentation volume from 195 to 245-degree angles.

Figure 4 has illustrated camera photos of bed topography variations in the laboratory for $U/U_c=0.98$. Figure 4-a depicts the tail area of the first upstream bend and the second downstream bend entrance up to the 235-degree angle. As it can be observed here, the scouring has occurred from the 165-degree angle at the tail area of the upstream bend to the junction between the two bends (area A1). It has continued to the 200-degree angle at the downstream inner bend entrance in area A2 (similar to the trend described in Figure 3-d). The scour has oriented towards the middle of the bend from the 195-degree angle. The scour at the downstream inner bend has continued to the 210-degree angle, after which sedimentation is observed (A3). There are also no variations observed in the vicinity of the downstream outer bend (A4). In Figure 4-b, bed topography variations in the first half of the downstream inner bend indicate sedimentation in area B1 from 217 to 280 degrees, while there is scour observed at mid-channel (B2). Area B3, near the outer bend, is still unchanged. Figure 4-c has illustrated topography variations from 250 to 310 degrees. Area C1, near the downstream inner bank, has undergone sedimentation, while area C2 in the middle of the bend is scoured. Sedimentation near the inner bend has oriented towards mid-channel from the 255-degree angle. In area C3, there are no identifiable variations in topography to the 290-degree angle; however, the shift in the flow direction at the 300-degree angle towards the outer bend entails scouring in this area. Figure 4-d depicts bed variations from 300 to 360-degree angles of the downstream bend. In area D1, near the inner bank, there are sedimentary stacks observed with an orientation towards the middle of the bend, and in area D2, scouring is found at the outer bend. As shown in these figures, the observations recorded about bed topography variations in the meandering channel in the laboratory are completely in line with the descriptions provided in Figure 3, particularly for $U/U_c=0.98$ in Figure 3-d.

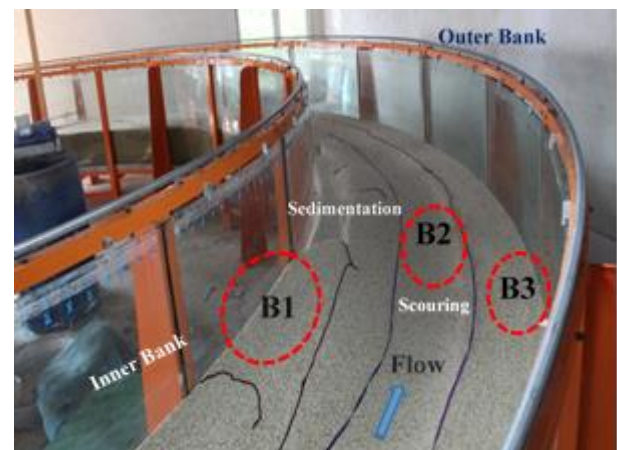
Table 1 has presented the amount of increase in the maximum scour and sedimentation values and the increase in the volume of sediment output at upstream and downstream bends for different ratios of U/U_c . There are various methods for calculating the sediment output volume, among which hydrography datasets and bathymetry data may be mentioned. Moreover, the application of different software programs, such as HEC-RAS, GSTARS3, Mike21, and Tecplot 360 [27], is one of the prevalent methods of calculating sediment volume. In this study, Tecplot 360 has been used for calculating the volume of sediment output. To this end, the collected data have been inserted into the software,

and after drawing bed topography, the volume of the sediments has been calculated using the integration command.

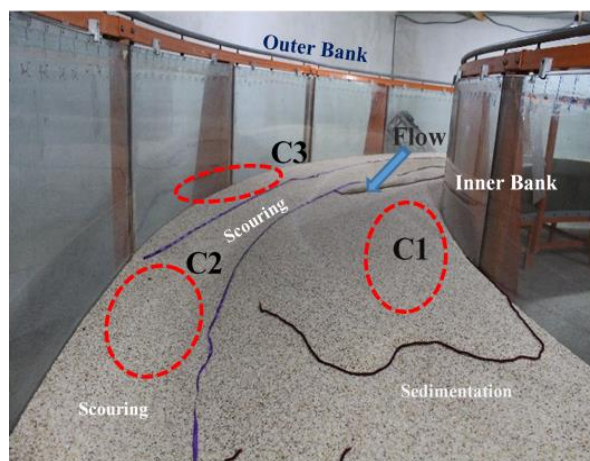
With this table taken into consideration, with an increase in U/U_c value from 0.89 to 0.92, 0.95, and 0.98, the volume of sediment output from the bend has increased by 38, 46, and 75 times respectively at the upstream bend. As shown here, the greatest variations related to the increased volume of the sediment output in both upstream and downstream bends occurs in the last case, where $U/U_c=0.98$ (which is the incipient motion of sediments on the upstream straight path). This can be attributed to the increase in the strength of eddies in this case.



(a)



(b)



(c)



(d)

Figure 4. Instances of bed topography variations in the laboratory for $U/U_c=0.98$ between (a) 165 and 235, (b) 217 and 280, (c) 250 and 310, and (d) 300 and 360 degrees.

3.2. Lateral Bed Profiles Variations

Figure 5 has illustrated variations in different lateral bed profiles from the beginning to the end of the upstream bend at 45, 90, 135, and 180-degree angles. A comparison between Figures 5-a, 5-b, and 5-c indicates that variations at the upstream bend have been highly insignificant, and only scour hole formation has been observed at the outer bend area, as in Figure 5-d. In Figure 5-d, approaching the end of the bend, the flow is

influenced by the downstream bend, and the bed topography variations have decreased at mid-channel. An increase in U/U_c from 0.75 to 0.86 has entailed trivial changes in bed topography at the upstream bend. As the flow is oriented towards the outer bank in the second half of the bend, increasing U/U_c from 0.89 to 0.98 causes scour hole formation from 0 to 40% of the channel width from the outer bend. The variations from mid-channel to the inner bank are insignificant.

Table 1. Comparison between variations in the maximum scour and sedimentation values for different U/U_c values in the meandering channel.

Bend location	U/U_c variations	Percentage of increase in the maximum sedimentation height (%)	Percentage of increase in the maximum scour depth (%)	Percentage of increase in the volume of sediment output (%)
Upstream bend	0.75-0.8	-	-	-
	0.8-0.84	-	-	-
	0.84-0.86	-	-	-
	0.86-0.89	-	-	-
	0.89-0.92	-	325	3693
	0.92-0.95	-	2.94	21.65
	0.95-0.98	-	245.7	62.95
Downstream bend	0.75-0.8	-	-	-
	0.8-0.84	200	50	33.5
	0.84-0.86	250	66.7	18.3
	0.86-0.89	119	100	30.1
	0.89-0.92	108.7	100	66.84
	0.92-0.95	2.08	20	90.65
	0.95-0.98	14.29	119.5	172.8

Instances of variations in lateral bed profiles from the beginning to the end of the downstream bend have been shown in Figure 6 at 225, 270, 315, and 360-degree angles. As shown in Figure 6-a, given the flow direction towards the inner bank in the first half of the bend, sedimentation has occurred at the inner bank. It has continued to a distance of approximately 20% of the channel width from the inner bank. The secondary flows also cause separation of sediments from the outer bank and mid-channel, whose result is scour hole generation at a distance of 20 to 60% from the outer bank. There are no variations found in bed topography in the rest of the channel width. At this angle, increasing U/U_c from 0.8 to 0.84, 0.86, 0.89, 0.92, and 0.98 has respectively increased the maximum sedimentation height by 2.5, 3, 6, 48, 47, and 41 times. With the same amount of increase in U/U_c , the maximum scour depth also increased by 1.5, 2, 3, 8, 16, and 22. In Figure 6-b, given the mid-channel flow orientation at the 270-degree angle, the sediments are gradually carried away from the inner bank. It can be observed that the maximum sedimentation has occurred within the range of 10 to 20% of the channel width from the inner bank. On account of this figure, sedimentation has continued to 30% of the channel width from the inner bank, and scour hole generation is observed at the distance of 35 to 75% from the inner bank. By increasing U/U_c from 0.8 to 0.84, and 0.86, the maximum sedimentation height remained unchanged at this angle, but increasing it to 0.89, 0.92, 0.95, and 0.98 increased the maximum sedimentation height by factors of 4, 7, 7.5, and 13, respectively.

Moreover, the maximum scour depth increased by 1.5, 2, 3, 4, 5, and 4.5 times respectively because of increasing U/U_c . In Figure 6-c, when the flow enters the second half of the downstream bend at the 315-degree angle and the helical flows decline, bed topography depends on the sediments carried downstream from the upstream bend. In the second half of the bend, the sediments have gradually been carried away from the inner bank and towards mid-channel. With the flow's orienting towards mid-channel and then towards the outer bank, scour hole generation has occurred from the mid-channel to the outer bank bend.

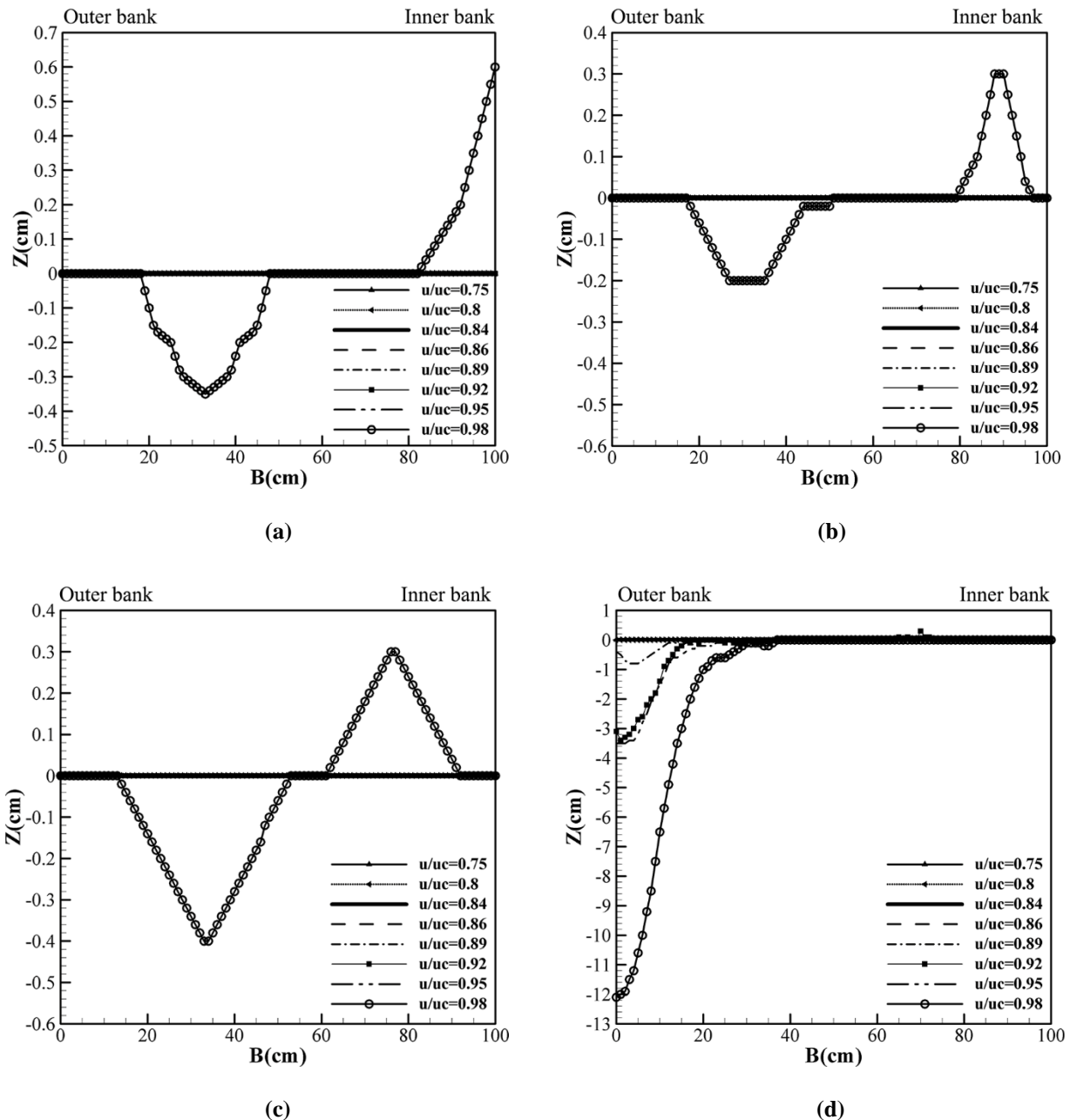


Figure 5. Instances of variations in the lateral bed profiles at (a) 45, (b) 90, (c) 135, and (d) 180-degree angles of the upstream bend.

A comparison between Figures 6-a to 6-c indicates that at the 225-degree cross-section, the maximum sedimentation has occurred at the inner bank, but at 270 and 315-degree cross-sections, with the shift in the flow orientation towards mid-channel and the

outer bank, the maximum sedimentation height has been observed from 10 to 20% of the channel width from the inner bank. The maximum sedimentation height has remained unchanged at the 315-degree cross-section with an increase in U/U_c value from 0.8 to 0.84 and 0.86, as was also the case with the 225-degree section. However, with an increase in U/U_c from 0.8 to 0.89, 0.92, 0.95, and 0.98, the maximum sedimentation height increased by 2, 4, 8, and 26 times. The maximum scour depth analysis indicates that increasing U/U_c from 0.8 to 0.84, 0.86, 0.89, and 0.92 did not change the value, but increasing it from 0.8 to 0.95 and 0.98 has increased the maximum scour depth by factors of 3 and 15.

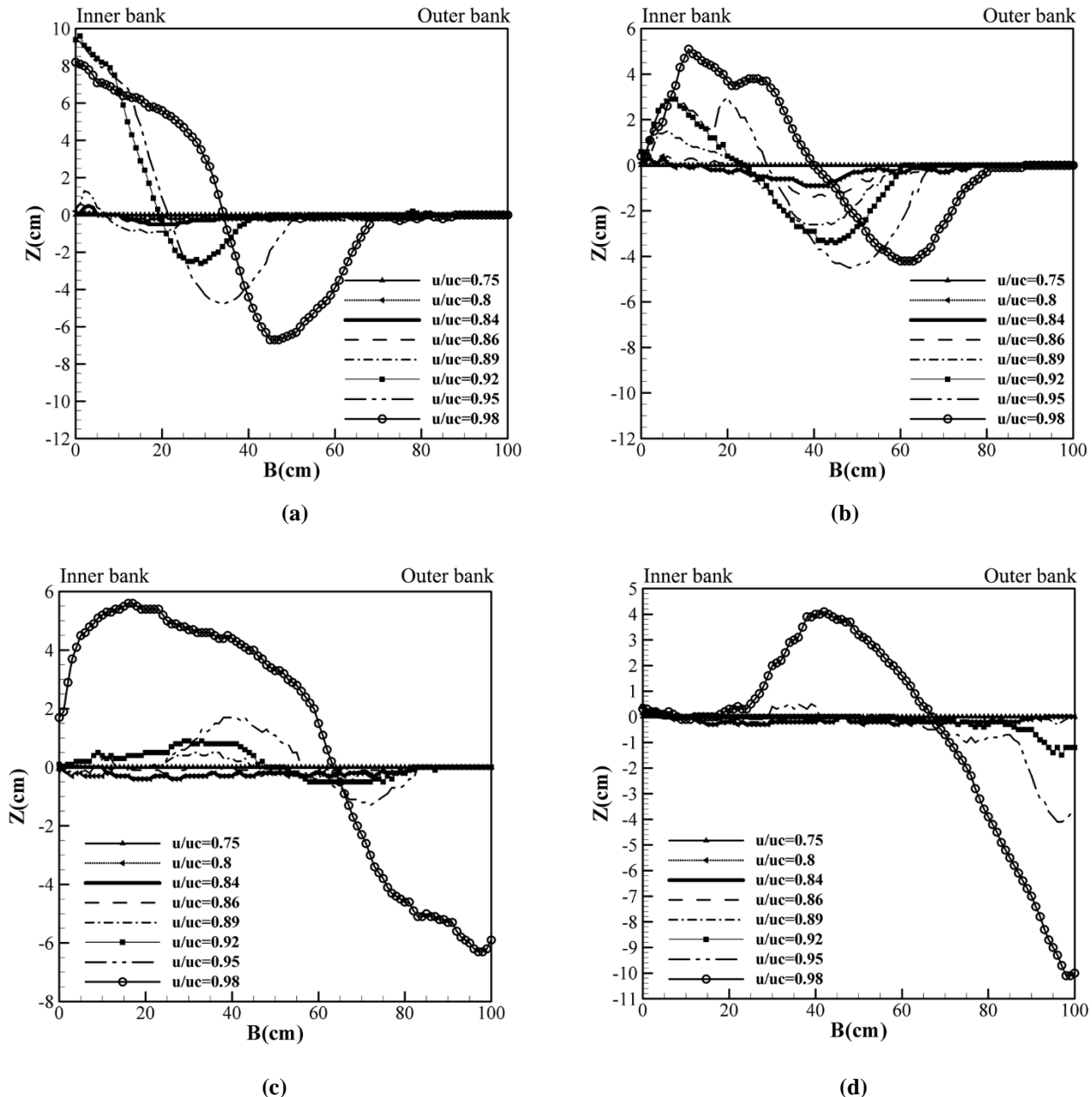


Figure 6. Instances of variations in the lateral bed profiles at (a) 225, (b) 270, (c) 315, and (d) 360-degree angles of the downstream bend.

In Figure 6-d, in experiments with $U/U_c=0.95$ and 0.98 , the sediments washed by the flow recede from the inner bank, are deviated towards mid-channel under the influence of the straight downstream path, and are deposited at the end of the bend, resulting in

accumulation of sedimentary stacks at the inner bend to mid-channel. There was insignificant sedimentation observed in the vicinity of the inner bank to mid-channel in other tests. In every test, bed topography variations at mid-channel have decreased closer and closer to the bend's tail area under the downstream straight path's effect on the flow. With the flow deviated towards the outer bank, the scour hole occurs at the mid-channel range to the outer bend. As shown in this figure, increasing U/U_c from 0.8 to 0.84, 0.86, and 0.89 does not change the maximum scour and sedimentation. Increasing U/U_c from 0.8 to 0.92, 0.95, and 0.98 has increased the maximum sedimentation height by 2, 2.5, and 20, while the maximum scour depth increased by respectively 5, 14, and 33 times.

3.3. Longitudinal Bed Profiles Variations

Figure 7 illustrates instances of different longitudinal bed profiles from the beginning to the tail area of the channel at distances of 10, 50, and 90% of the channel width from the inner bank for different cases. According to this figure, most bed topography variations have occurred from the tail area of the upstream bend to the end of the downstream bend. As shown in Figure 7-a, bed topography had trivial variations at the upstream bend's outer bank. As the flow is oriented towards the outer bank in the second half of the upstream bend, the maximum scour hole has been created within the range of 180 to 200 degrees. In this figure, sedimentation occurred from a range of 10% of the channel width from the inner bank at the 220-degree angle to the end of the downstream bend. It is intensified in the first half of the bend, where the maximum value has occurred within the range of 240 to 260 degrees. These sedimentary stacks have been carried downstream gradually away from the inner bank and towards mid-channel.

Figure 7-b illustrates how insignificant bed topography variations are from mid-channel to the area short of the downstream bend. The flow is oriented towards the inner bank at the beginning of the downstream bend. The sediments washed out of the scour hole created in that area join the sediments deposited from the upstream sections and head downstream. With the bend geometry taken into consideration, the flow orientation has gradually shifted away from the inner bank and directed towards mid-channel and then towards the outer bank in the second half of the bend. Shifted towards mid-channel in the second half of the bend, the flow sheds over the sedimentary stacks, creating a scour hole at mid-channel within the range of 220 to 300 degrees. The sediments washed out of the scour hole have joined the sediments deposited from upstream, and they have been observed headed downstream. In time, these stacks and holes move towards the outer bank and then through the downstream straight path, leading to the discharge of sediments from the bend.

As shown in Figure 7-c, the scour is intensified at the outer bank and the second half of the bend, and its maximum has occurred within the range of 300 to 360 degrees. The whole trend described in Figure 7 is also visible in Figure 3 (bed topography variations) and Figure 5 (variations in the lateral profile) within the same ranges as those in this case.

An overall review of the results of bed topography variations along the meandering channel indicated that increasing U/U_c from 0.89 to 0.92, 0.95, and 0.98 has increased the maximum scour depth at the upstream bend by factors of 4.3, 4.4, and 15, respectively. Increasing U/U_c from 0.8 to 0.84, 0.86, 0.89, 0.92, 0.95, and 0.98 at the downstream bend has increased the maximum scour depth by respectively 1.5, 2.5, 5, 10, 12, and 26 times. Moreover, the maximum sedimentation also increased by factors of 3, 10, 23, 48, 49, and 56 due to the increase in this ratio.

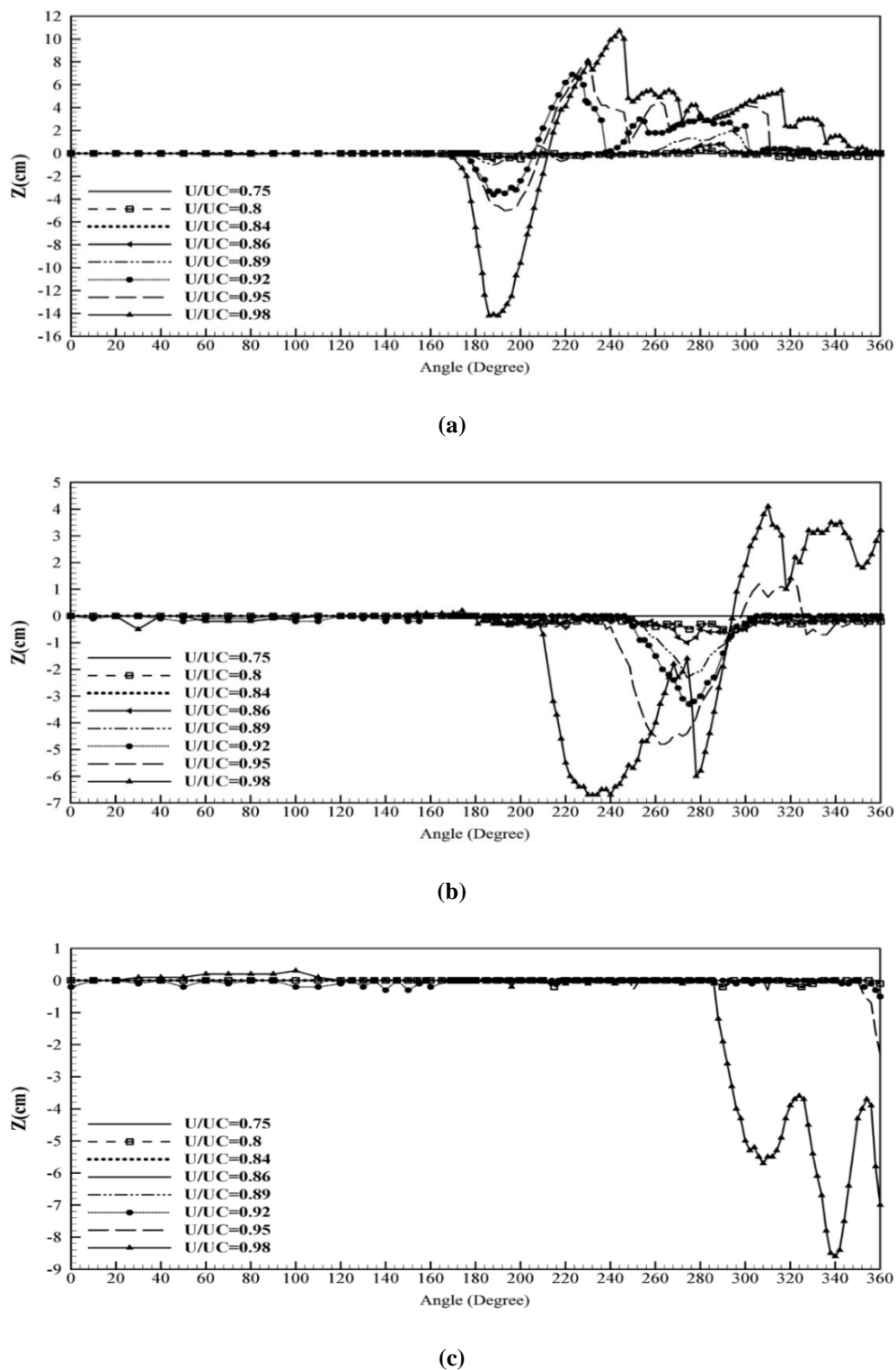


Figure 7. Instances of variations in the longitudinal bed profile at distances of (a) 10% of the channel width from the first outer bend and the second inner bend, (b) 50% of the channel width, and (c) 90% of the channel width from the first inner bend and the second outer bend.

3.4. Qualitative Flow Pattern

Figure 8 illustrates instances of the flow's qualitative behavior at the upstream and downstream bends in the meandering channel using colored ribbons (a purple ribbon at

the layer near the water surface and a yellow ribbon at the layer near the bed). Figures 8-a and 8-b respectively depict sections from the first and the second halves of the upstream bend. Flow orientations towards the inner bend at the layers near the bed and towards the outer bend at the upper layers are evident in these figures. Figure 8-c illustrates the beginning of the downstream bend. As shown in this figure, since the inner and outer bends swap positions compared to the upstream bend at the downstream bend inlet, the streamlines are again oriented towards the outer bank at the water surface. Figure 8-d has depicted the flow at the end of the downstream bend. According to this figure, from approximately the 190-degree angle, the upper layers' flow is oriented from the outer bend towards mid-channel. After the 300-degree angle, it is mostly influenced by the straight downstream path. This flow variations trend is in line with the descriptions provided in Figure 3 with respect to bed topography variations.

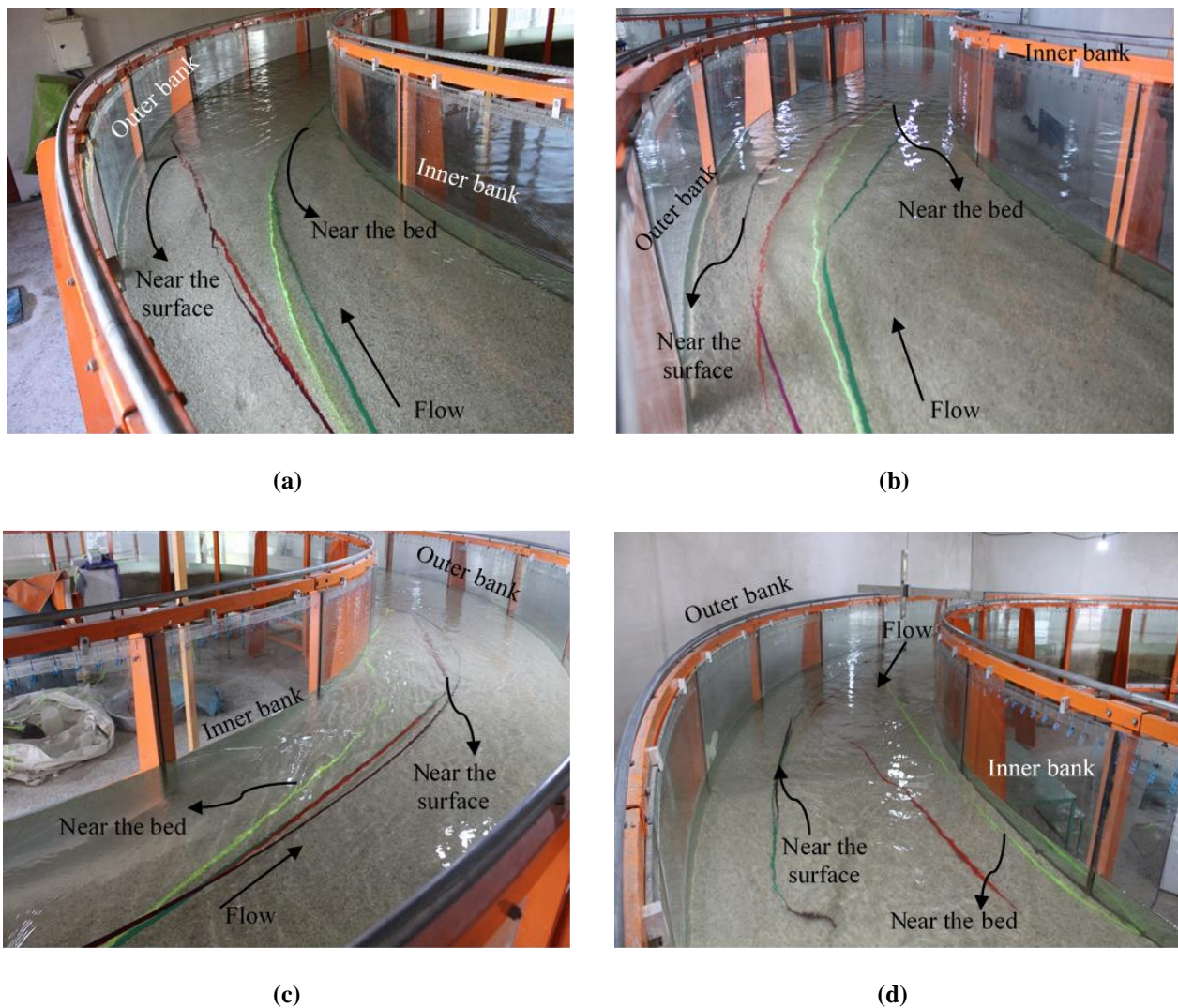


Figure 8. Instances of the qualitative flow behavior at the upstream and downstream bends of the meandering channel for $U/U_c=0.98$ at (a) the upstream bend inlet, (b) the upstream bend outlet, (c) the downstream bend inlet, and (d) the downstream bend outlet.

3D view of the streamlines at the layers near the bed and those near the water surface along the meandering channel, as well as the helical flows [28] created along the path, are schematically shown in Figure 9. As shown in this figure, the flow orientation near the water surface is shifted towards the outer bend, and that at the layer near the bed is shifted

towards the inner bend. Also, the presence of helical flows in the bend has created scour in the vicinity of the outer bend and sedimentation near the inner bend. These bed topography variations, which are affected by the presence of helical flows at the downstream bend for $U/U_c=0.98$, have been described in Figure 3-d. Analysis of the qualitative flow pattern in Figure 8, the schematic illustration of the flow pattern in Figure 9, and the scour and sedimentation patterns in Figure 3 refer to the correspondence between the scour changes imposed on the meandering channel bends and the flow pattern. Moreover, the vector is drawn in the figure also matches the streamlines presented by Vaghefi et al. [29] and Akbari and Vaghefi [30] at the layers near the bed (towards the inner bend) and the layer near the water surface (towards the outer bend) in a 180-degree sharp bend with $R/B=2$. In addition, flow pattern variation in the meandering channel and its relationship with the camera photo of bed scour pattern variation in the laboratory under incipient motion condition in the first bend for $U/U_c=0.98$ are well illustrated in Figure 4.

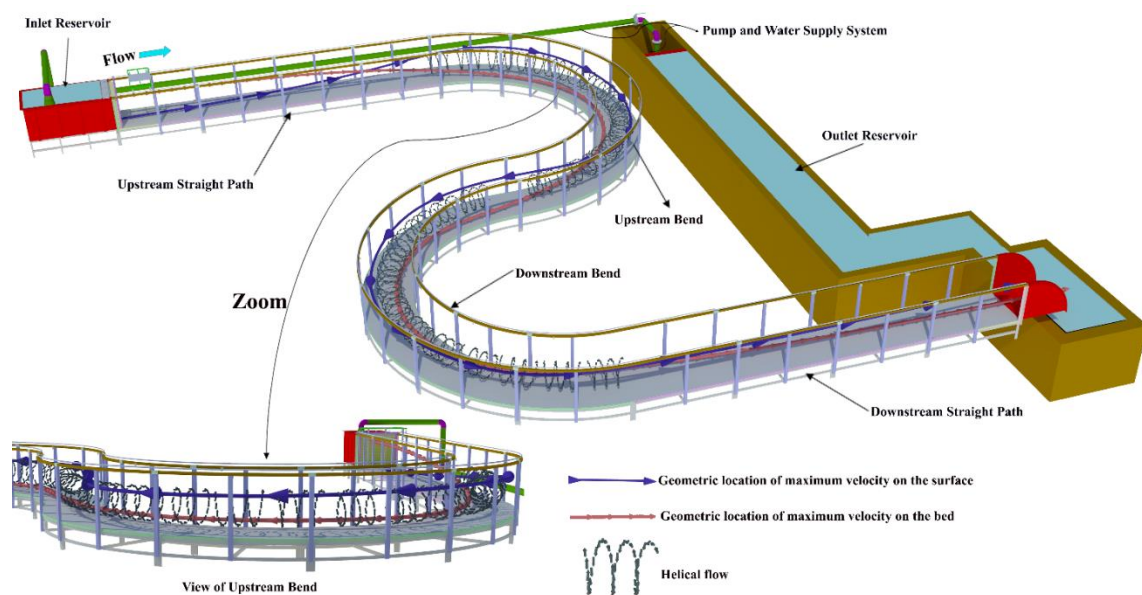


Figure 9. A schematic illustration of the 3D flow pattern at the layers near the bed and the water surface in the meandering channel.

4. Conclusions

This paper presented the experiments conducted for different mean velocity to critical velocity ratios (U/U_c) at the straight upstream path to determine the incipient motion conditions in a meandering channel with two consecutive 180-degree mild bends. A study of bed topography variations along the meander, the effect of the upstream bend geometry on downstream bend bed topography variations, and the effect of the downstream straight path on the upstream bend are among the points addressed in this study. The following is a summary of the results obtained from this study:

- Bed topography variations at the upstream bend suggest the effectiveness of the downstream bend in altering the incipient motion conditions along this bend. In addition to the downstream straight path's role in altering the incipient motion conditions, the upstream bend's geometry has also affected bed topography variations at the downstream bend.
- For $U/U_c=0.89$ to 0.98 in both bends, bed topography changed under the bend geometry's influence. The reduction of water level at the upstream bend resulted in an increase in the flow velocity compared to that at the upstream straight path. The downstream bend also showed more bed topography variations than the upstream bend, given its greater water level reduction than the first bend. For $U/U_c=0.89$ to 0.95 at the first bend, however, no sedimentation occurred.

- Since the flow at the first half of the downstream bend is oriented towards the inner bank, the maximum sedimentation height for every U/U_c value also occurred at a distance from 0 to 5% from the inner bank. Increasing $U/U_c = 0.8$ to 0.98 changed the location of the maximum sedimentation from the 195-degree angle to the 245-degree angle.
- For every U/U_c at the upstream bend, the maximum scour occurred at a distance of 5% of the channel width from the outer bank and within the range of 178 to 180 degrees. Increasing U/U_c from 0.89 to 0.92, 0.95, and 0.98 at this bend respectively increased the maximum scour depth by factors of 4.3, 4.4, and 15.
- Increasing U/U_c from 0.8 to 0.84, 0.86, 0.89, 0.92, 0.95, and 0.98 at the downstream bend respectively increased the maximum scour depth by factors of 1.5, 2.5, 5, 10, 12, and 26, and the maximum sedimentation height by factors of 3, 10, 23, 48, 49, and 56.
- For U/U_c values ranging from 0.8 to 0.89 at the downstream bend, the maximum scour occurred at the distance of 30 to 40% of the channel width within the range of 270 to 275 degrees. However, for U/U_c values ranging from 0.92 to 0.98, the maximum scour was relocated to a distance equal to 5% of the channel width from the inner bank within the range of 185 to 195 degrees.

Author Contributions

N. M.

Designing and constructing the laboratory setup; Data Collection; Methodology; Visualization; Writing-Original Draft; Resources; Formal analysis; Software; Investigation

S. H. M.

Supervision; Conceptualization; Project administration; Formal analysis; Validation; Writing-Reviewing, and Editing

M. V.

Supervision; Designing the laboratory setup; Conceptualization; Methodology; Project administration; Formal analysis; Validation; Writing-Reviewing, and Editing

A. K.

Advising, Formal analysis; Conceptualization; Investigation; Validation; Writing-Reviewing, and Editing

All authors participated in final review and editing of the paper.

Funding

This research received no external funding.

Conflicts of Interest

The authors declare no conflict of interest.

References

1. Randle, T.J. Use of Multidimensional Models to Investigate Boundary Shear Stress through Meandering River Channels. *Water* **2020**, *12*, 3506.
2. Bertalan, L.; Novák, T.J.; Németh, Z.; Rodrigo-Comino, J.; Kertész, Á.; Szabó, S. Issues of meander development: land degradation or ecological value? The example of the Sajó River, Hungary. *Water* **2018**, *10*, 1613.

3. Garcia, J.T.; Castillo, L.G.; Haro, P.L.; Carrillo, J.M. Occlusion in Bottom Intakes with Circular Bars by Flow with Gravel-Sized Sediment. An Experimental Study. *Water* **2018**, *10*, 1699.
4. Das, V.K.; Barman, K.; Roy, S.; Chaudhuri, S.; Debnath, K. Near bank turbulence of a river bend with self similar morphological structures. *Catena* **2020**, *191*, 104582.
5. Shields, A. *Application of the Theory of Similarity and Turbulence Research to the Bedload Movement*. Transl. QM Saleh. Mitt. Preuss. Vers. Wasserbau Schiffbau: Berlin, Germany, 1936.
6. Dey, S.; Papanicolaou, A. Sediment threshold under stream flow: A state-of-the-art review. *KSCE. J. Civ. Eng.* **2008**, *12*, 45-60.
7. Kramer, H. Sand mixtures and sand movement in fluvial model. *Trans. Am. Soc. Civ Eng.* **1935**, *100*, 798-838.
8. Bagnold, R.A. The nature of saltation and of 'bed-load' transport in water. Proceedings of the Royal Society of London. *A. Math. Phys. Sci.* **1973**, *332*, 473-504.
9. Neill, C.R. Note on initial movement of coarse uniform bed-material. *J. Hydraul. Res.* **1968**, *6*, 173-176.
10. Lavelle, J.W.; Mofjeld, H.O. Do critical stresses for incipient motion and erosion really exist?. *J. Hydraul. Eng.* **1987**, *113*, 370-385.
11. Yen, C.L.; Lee, K.T. Bed topography and sediment sorting in channel bend with unsteady flow. *J. Hydraul. Eng.* **1995**, *121*, 591-599.
12. Dey, S.; Debnath, K. Influence of streamwise bed slope on sediment threshold under stream flow. *J. Irrig. Drain. E.* **2000**, *126*, 255-263.
13. Xu, D.; Bai, Y. Experimental study on the bed topography evolution in alluvial meandering rivers with various sinuousnesses. *J. Hydro-Env. Res.* **2013**, *7*, 92-102.
14. Mohtar, W. Threshold criteria for incipient grain motion with turbulent fluctuations on a horizontal bed. *Sains. Malay.* **2015**, *44*, 147-153.
15. Liu, X.; Zhou, Q.; Huang, S.; Guo, Y.; Liu, C. Estimation of flow direction in meandering compound channels. *J. Hydrol.* **2018**, *556*, 143-153.
16. Qin, C.; Shao, X.; Xiao, Y. Secondary Flow Effects on Deposition of Cohesive Sediment in a Meandering Reach of Yangtze River. *Water* **2019**, *11*, 1444.
17. Azarisamani, A.; Keshavarzi, A.; Hamidifar, H.; Javan, M. Effect of Rigid Vegetation on Velocity Distribution and Bed Topography in a Meandering River with a Sloping Bank. *Arab. J. Sci. Eng.* **2020**, *45*, 8633-8653.
18. Akbari, M.; Vaghefi, M.; Chiew, Y.M. Effect of T-shaped spur dike length on mean flow characteristics along a 180-degree sharp bend. *J. Hydrol. Hydromech.* **2021**, *69*, 98-107.
19. Moghaddassi, N. *Experimental study of scour pattern around bridge piers in meander*. Ph.D. dissertation, Islamic Azad University, Science and Research Branch: Tehran, Iran, 2021.
20. Leschziner, M.A.; Rodi, W. Calculation of strongly curved open channel flow. *J. Hydraul. Div.* **1979**, *105*, 1297-1314.
21. Raudkivi, A.J.; Ettema, R. Clear-water scour at cylindrical piers. *J. Hydraul. Eng.* **1983**, *109*, 338-350.
22. Ben Mohammad Khajeh, S.; Vaghefi, M.; Mahmoudi, A. The scour pattern around an inclined cylindrical pier in a sharp 180-degree bend: an experimental study. *Int. J. River. Basin. Manag.* **2017**, *15*, 207-218.
23. Chiew, Y.M. Scour protection at bridge piers. *J. Hydraul. Eng.* **1992**, *118*, 1260-1269.
24. Termini, D. Experimental observations of flow and bed processes in large-amplitude meandering flume. *J. Hydraul. Eng.* **2009**, *135*, 575-587.
25. Vaghefi, M.; Motlagh, M.J.T.N.; Hashemi, S.S.; Moradi, S. Experimental study of bed topography variations due to placement of a triad series of vertical piers at different positions in a 180 bend. *Arab. J. Geosci.* **2018**, *11*, 102-115.
26. Asadollahi, M.; Vaghefi, M.; Akbari, M. Effect of the position of perpendicular pier groups in a sharp bend on flow and scour patterns: numerical simulation. *J. Braz. Soc. Mech. Sci.* **2020**, *42*, 422-437.
27. Solati, S.; Vaghefi, M.; Behrooz, A.M. Effect of Duration and Pattern of Hydrographs on Scour Around Pier in Sharp Bend Under Incipient Motion and Live Bed Conditions. *Int. J. Civ. Eng.* **2021**, *19*, 51-65.
28. Ben Meftah, M.; De Padova, D.; De Serio, F.; Mossa, M. Secondary Currents with Scour Hole at Grade Control Structures. *Water* **2021**, *13*, 319.
29. Vaghefi, M.; Akbari, M.; Fiouzi, A.R. An experimental study of mean and turbulent flow in a 180 degree sharp open channel bend: Secondary flow and bed shear stress. *KSCE. J. Civ. Eng.* **2016**, *20*, 1582-1593.
30. Akbari, M.; Vaghefi, M. Experimental investigation on streamlines in a 180° sharp bend. *Acta. Sci-Tech.* **2017**, *39*, 425-432.